MULTIMODAL IMAGING AND MULTIFOCAL ELECTRORETINOGRAPHY DEMONSTRATE AUTOSOMAL RECESSIVE STARGARDT DISEASE MAY PRESENT LIKE OCCULT MACULAR DYSTROPHY

ROBERT A. SISK, MD,*†‡ THEODORE LENG, MD§

Purpose: To describe multimodal imaging and electrophysiologic characteristics of an unusual subset of patients with genetically confirmed autosomal recessive Stargardt disease (STGD1) who exhibited a central form of cone dysfunction resembling occult macular dystrophy that preceded the development of lipofuscin flecks, atrophy of retinal pigment epithelium (RPE), or full-field electroretinography abnormalities.

Methods: Retrospective, observational descriptive case series.

Results: Five patients with compound heterozygous ABCA4 mutations presented with bilateral visual acuity reduction, normal-appearing fundi, and blocked choroidal fluorescence on fluorescein angiography. One sibling each of two probands with identical genotypes was also included for analysis. Full-field electroretinography testing was normal in all patients, but multifocal electroretinography demonstrated centripetally depressed amplitudes exceeding areas of fundus autofluorescence, infrared imaging, and spectral domain optical coherence tomography abnormalities. Spectral domain optical coherence tomography initially revealed disruption of the inner segment ellipsoid band accompanying an ovoid hypofluorescent foveolar lesion. Progression to later stages was accompanied by the loss of the foveal photoreceptor outer segments, creating foveal cavitation with preservation of the RPE. Fundus autofluorescence and infrared imaging demonstrated corresponding bull's eye lesions. Over time, the foveal potential space on spectral domain optical coherence tomography collapsed, and three patients developed RPE atrophy and visible lipofuscin flecks. The flecks were detectable by fundus autofluorescence and infrared imaging earlier than by biomicroscopy. From these findings, a staging system for this subset of Stargardt disease presenting with central cone dysfunction was developed and presented herein.

Conclusion: Autosomal recessive Stargardt disease may present as a central cone dysfunction syndrome before the development of lipofuscin flecks, atrophy of RPE, or full-field electroretinography abnormalities. If emerging therapies for Stargardt disease succeed, early recognition and treatment of patients with preserved foveal photoreceptor and RPE cell bodies may yield a more favorable visual prognosis.

RETINA 34:1567–1575, 2014

Stargardt disease is the most common juvenile macular dystrophy.[1] Ninety percent of cases with Stargardt disease originate from autosomal recessive mutations in the ABCA4 gene (STGD1). ABCA4 encodes a transmembrane channel, ATP-binding cassette transporter (ABCR), which functions as a flippase and prevents retinoids from accumulating within the disk membranes of photoreceptor outer segments.[2,3] Mutations in ABCA4 result in dysfunction of the photoreceptors and retinal pigment epithelium (RPE) and lipofuscin accumulation that preferentially affects the central retina.[4–7] In addition to Stargardt disease, mutations in ABCA4 have been attributed to cases of age-related maculopathies, cone–rod dystrophy, and retinitis

pigmentosa.[8–11] Despite extensive clinical experience, the role of the ABCA4 gene in producing retinal disease remains incompletely described. Several studies contradict each other regarding which mutations in ABCA4 are pathogenic or benign.[12–14] Despite a 1 in 10,000 incidence, up to 5% of people of northern European ancestry harbor pathologic mutations in ABCA4 in 1 allele, exceeding the anticipated carrier rate, suggesting other genetic interactions may play a significant role in manifestations of disease.[15–17]

Several phenotypic classification systems for STGD1 have been proposed based on funduscopic characteristics and electrophysiologic findings.[18–21] However, currently, no system adequately describes all phenotypic presentations, especially those patients who present without lipofuscin flecks, atrophy of the RPE, or full-field electroretinography (ffERG) abnormalities. Fishman et al[18] divided patients into three phenotypes, although all patients had flecks or RPE atrophy. In his celebrated *Stereoscopic Atlas of Macular Diseases*, Dr. J. Donald Gass classified Stargardt disease into four phenotypes based on funduscopic and full-field electrophysiologic findings: 1) vermillion fundi and hidden choroidal fluorescence (without flecks); 2) atrophic maculopathy with or without flecks; 3) atrophic maculopathy with late signs and symptoms of retinitis pigmentosa; and 4) flecks not associated with macular atrophy (fundus flavimaculatus).[21] Although Gass' classification described patients with Type 3 Stargardt disease resembling retinitis pigmentosa, their presentation more closely resembles cone–rod dystrophy.[9] Macular disease occurs early and rod responses remain measurable until an end stage. Most patients with Stargardt disease from ABCA4 mutations present with Type 2 disease, and therefore, available phenotypic classifications most adequately describe this cohort. Consequently, most reports describing natural history, anatomical descriptions, imaging, and electrophysiologic correlates for Stargardt disease involve patients with Type 2 disease. We report previously undescribed spectral domain optical coherence tomography (SD-OCT), infrared imaging, and fundus autofluorescence (FAF) findings of Gass' Type 1 Stargardt disease, those without flecks, RPE atrophy, or ffERG abnormalities, whose phenotype resembles occult macular dystrophy (OMD), a localized central form of cone dystrophy. The results will challenge the adequacy of the current phenotypic classification systems and lend argument toward further development of a primarily genetic classification.

Recent success using gene replacement therapy in treating patients with Leber Congenital Amaurosis (LCA) Type 2 has set the stage for additional human studies involving other human retinal dystrophies including Stargardt disease.[22,23] The findings described in this report will support candidacy for patients with Stargardt disease without atrophic maculopathy for gene replacement therapy and may facilitate earlier identification and improved selection of candidates for this and other treatment approaches.

Methods

The records of all patients of the pediatric retina service at Cincinnati Children's Hospital Medical Center, the Retina Division of the Cincinnati Eye Institute, and the Byers Eye Institute at Stanford University who presented with Stargardt disease between September 1, 2009 and August 31, 2012 were retrospectively reviewed. Records from outside providers who previously cared for these patients were also reviewed. Patients meeting the Gass' clinical description of Type 1 Stargardt disease, vermillion fundi without flecks, with or without blocked choroidal fluorescence on fluorescein angiography (FA), and having at least one known disease-causing ABCA4 mutation were included.[21] All biologic parents were examined and confirmed to be without ABCA4-related retinal disease. Genetic analysis was performed through a CLIA-certified laboratory (Carver Lab, Iowa City, IA or EyeGENE [The National Ophthalmic Disease Genotyping and Phenotyping Network], National Eye Institute, Bethesda, MD) on all individuals with sporadic presentation and on at least one individual within the same generation when siblings were affected.

Of patients meeting inclusion criteria, those with generalized cone dysfunction on ffERG, indicating cone or cone–rod dystrophy, were excluded. Patients with lipofuscin flecks by funduscopy or foveal RPE atrophy, consistent with Stargardt disease other than Gass' Type 1, were initially excluded. Two patients with Type 1 disease were identified by older sibling probands with Gass' Type 2 disease. After confirming identical genotypes, these two patients were also

From the *Cincinnati Eye Institute, Cincinnati, Ohio; †Cincinnati Children's Hospital Medical Center, Cincinnati, Ohio; ‡Department of Ophthalmology, University of Cincinnati, Cincinnati, Ohio; and §Byers Eye Institute, Stanford University School of Medicine, Palo Alto, California.

Paper presented at the 2012 Association of Pediatric Retinal Surgeons Meeting, Park City, UT, September 23, 2012, and at the 46th Annual Retina Society Meeting, Beverly Hills, CA, September 23, 2013.

None of the authors have any financial/conflicting interests to disclose.

Reprint requests: Robert A. Sisk, MD, Cincinnati Eye Institute, 1945 CEI Drive, Cincinnati, OH 45242; e-mail: rsisk@cincinnatieye.com

included for analysis. Neither of the younger siblings had funduscopically evident flecks, but one had bilateral foveal RPE atrophy.

Each patient underwent complete ocular examination with best-corrected visual acuity, slit-lamp examination, and indirect ophthalmoscopy. Ancillary testing included a variable combination of multimodal retinal imaging, multifocal electroretinography (mfERG), and ffERG (Diagnosys D218, Software V6.0.47 with 61 hexagon array, Diagnosys LLC, Lowell, MA). Multimodal imaging was performed by confocal scanning laser ophthalmoscope (cSLO) using a Heidelberg Spectralis HRA-OCT (Heidelberg Engineering, Dossenheim, Germany) that included FAF, FA, infrared imaging, and SD-OCT (Figure 1). The high-resolution horizontal 5-line raster and 6 mm × 6 mm cube scan protocols were used to correlate SD-OCT with FAF and infrared imaging features. Fundus autofluorescence was stimulated by argon blue laser (488 nm) and emission was filtered above 500 nm to reduce contributions from the crystalline lens. A series of FAF images was averaged to reduce noise and artifacts and increase image resolution. The confocal detection unit uses a 400-μm pinhole aperture to suppress light from above or below the confocal plane. The scanning field was 30°. To avoid contaminating the FAF imaging with residual hyperfluorescence from previous FA examinations, the FAF examination was performed before FA imaging. We compared the features of ophthalmoscopy with the multimodal imaging performed using the HRA-OCT unit. Multifocal electroretinography and ffERG were performed as per ISCEV standards.[24,25]

Statistical analysis was performed with Microsoft Excel 2011 (Microsoft Corp., Redmond, WA). Snellen best-corrected visual acuities were converted to logMAR best-corrected visual acuities for statistical analysis.

Results

Five patients, 3 female and 2 male, met the initial inclusion criteria for Gass' Type 1 Stargardt disease. Two older sibling probands with flecks or RPE atrophy who had identical genotypes to their younger siblings were also included for analysis. Baseline characteristics and genetic data of all patients are

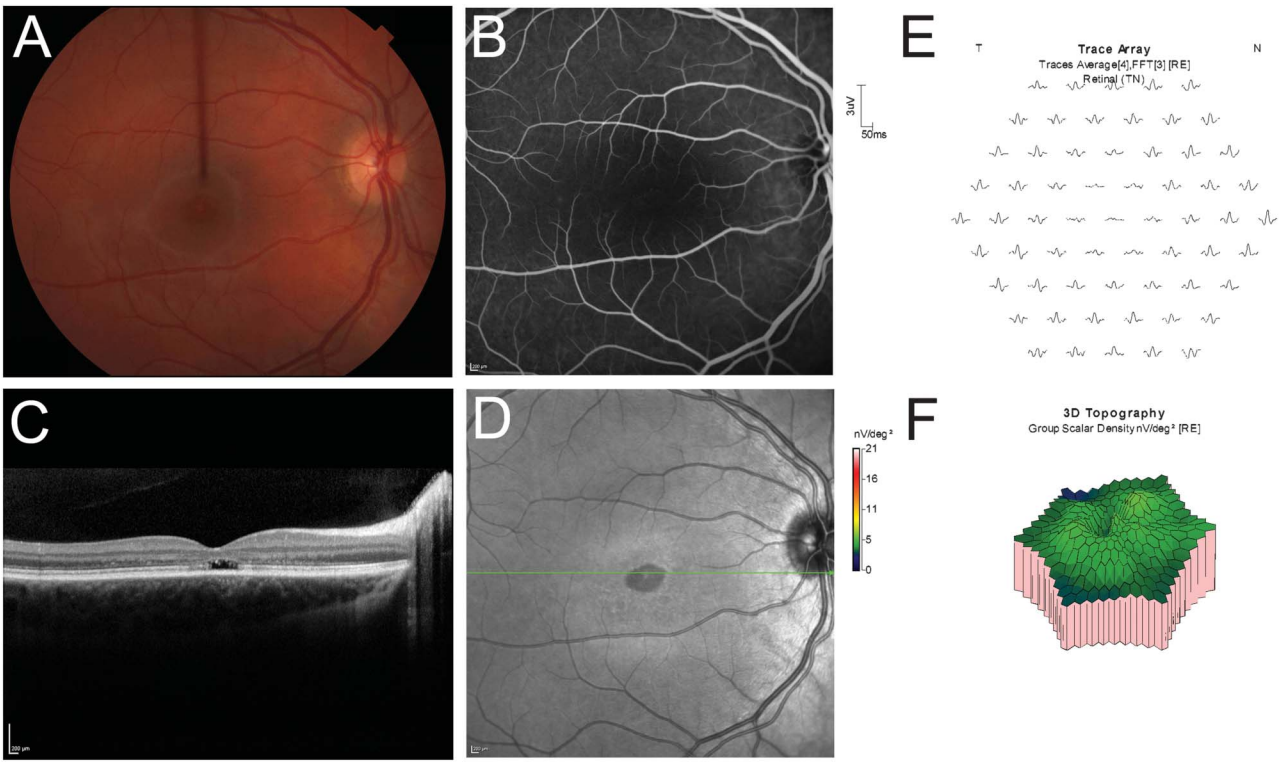

Fig. 1. Multimodal imaging (**A–D**) and mfERG (**E** and **F**) of the right eye of Patient 2, a 15-year-old boy with Stage 3 disease. Visual acuity was 20/80. **A.** Color fundus photograph demonstrates brick red oval area at the fovea with mild blunting of foveal light reflex. **B.** Fluorescein angiography demonstrates blocked choroidal fluorescence and very faint oval foveal hyperfluorescent window defect. Late frames were unchanged. **C.** Spectral domain optical coherence tomography horizontal raster image through the foveola showed foveal cavitation with dangling residual foveal outer segments. The RPE band seemed normal without transmission defects into the choroid. **D.** Infrared imaging highlighted the abnormality on color photography and demonstrated surrounding coarseness within a surrounding hyperintense ring. **E.** Trace array of mfERG with abnormalities extending far beyond the foveal abnormalities demonstrated by the multimodal imaging. **F.** Topographic representation shows the loss of foveal and parafoveal peak.

Table 1. Baseline Demographics and Genetic Information

Patient	Sex	Age at Onset, years	Family History	Follow-up, days	Pathologic ABCA4 Mutation #1	Pathologic ABCA4 Mutation #2	ABCA4 Mutations of Unknown Significance
1	F	13.1	Adopted	720	Gly1961Glu	Val1973del1ggaG	—
2	M	15.6	No	819	Val256Val c768G > T	p.Arg1300Gls c3899G > A	pGly991Arg c2971 G > C
3	F	10.1	Yes*	413	Gln 1135 Stop	Gly863Ala	Cys2150Tyr
4	F	7.2	Yes*	0	Gln1135 Stop	Gly863Ala	Cys2150Tyr
5	F	12.1	Yes†	610	C1490Y	IVS40+5 G > A	—
6	F	10.6	Yes†	147	C1490Y	IVS40+5 G > A	—
7	M	25.0	No	0	Gly1961Glu	Unidentified	—

*Patients 3 and 4 are siblings.
†Patients 5 and 6 are siblings.
F, female; M, male.

recorded in Table 1. Median age at presentation was 12.1 years (range, 7.2–25.0 years), and patients were followed for a median of 14 months (range, 0–27 months). All patients had pathologic mutations in ABCA4 on both alleles except Patient 7. In the remaining six patients, compound heterozygous ABCA4 mutations were identified—one allele produced a nonsense mutation and the other produced a missense mutation. No unrelated patients shared both mutated ABCA4 alleles.

Visual acuity data, multimodal imaging, and mfERG findings applicable for each patient are recorded in Table 2. Best-corrected visual acuity remained stable or no worse throughout follow-up in all but two patients ($P = 0.73$). All tested patients had central depression of N1-P1 amplitudes with increased implicit times on mfERG. Visual acuity loss was positively correlated with greater reduction in amplitudes, longer implicit times, and larger area of central waveforms affected. The area of mfERG waveform abnormalities exceeded corresponding areas of FAF and SD-OCT abnormalities, indicating functional photoreceptor disturbances preceded and exceeded evident in vivo anatomical changes. Visual acuity reduction was associated with greater alteration of foveal photoreceptor anatomy by SD-OCT central raster scans and greater FAF changes in all patients. Fundoscopic, imaging, and electrophysiologic findings were symmetrical in all patients. Patients 1 and 6 had observed deterioration of foveal architecture on SD-OCT during follow-up that was used to create a model for staging disease progression in patients with Stargardt disease resembling OMD described in Table 3 and Figure 2.

All patients had symmetrical ovoid foveal FAF abnormalities. Those eyes with either disruption of the inner segment ellipsoid band (Stage 1) or loss of foveal outer segments but with preservation of photoreceptor cell bodies on SD-OCT raster scans (Stage 2) displayed foveolar hypoautofluorescence. Those with the absence of foveal photoreceptor cell bodies, development of a confluent potential space replacing foveal outer segments (Stage 3), and preservation of the Müller cell framework and RPE band integrity had central isoautofluorescence surrounded by a bull's eye configuration of alternating rings of hyperautofluorescence, hypoautofluorescence, and a fainter second ring of hyperautofluorescence, centrifugally. Collapse of the potential space on SD-OCT (Stage 4) in Patient 1 did not result in FAF changes. Eyes with irregularities or thinning of the RPE band (Stage 5) had central hypoautofluorescence in a bull's eye configuration and multifocal punctate hyperautofluorescent spots outside the inner ring of hyperautofluorescence. Older siblings with typical Type 2 Stargardt disease had larger, ovoid central

Table 2. Visual Acuity, Multimodal Imaging, and mfERG Data

Patient	Eye	Baseline VA	Final VA	Stages Observed*	FAF*	IR*	SD-OCT*	FA*	mfERG*
1	OD	20/30	20/100	3, 4	Y	Y	Y	Dark choroid	Reduced centripetally 0° to 20°
	OS	20/100	20/100					Window defect at the fovea	
2	OD	20/80	20/80	3	Y	Y	Y	NT	Reduced centripetally 0° to 20°
	OS	20/70	20/70						
3	OD	20/100	20/70	5, 6	Y	Y	Y	NT	NT
	OS	20/125	20/100						
4	OD	20/25	20/25	2	Y	Y	Y	NT	NT
	OS	20/25	20/25						
5	OD	20/80	20/80	5, 6	Y	Y	Y	Dark choroid	Reduced centripetally 0° to 30°
	OS	20/80	20/100					Bull's eye lesion at fovea Focal macular lesions	
6	OD	20/25	20/25	1, 2	Y	Y	Y	NT	Reduced centripetally 0° to 20°
	OS	20/25	20/25						
7	OD	20/60	20/60	3	Y	Y	Y	NT	NT
	OS	20/80	20/80						

*Findings were symmetrical between eyes of the same patient.
IR, infrared imaging; NT, not tested; VA, visual acuity; Y, yes, abnormal.

hypoautofluorescence surrounded by a hyperautofluorescent ring and numerous, discrete focal hyperautofluorescent thickenings of the RPE band throughout the remaining macula (Stage 6). Infrared imaging demonstrated more widespread distribution of flecks than FAF.

Discussion

ABCA4 encodes a flippase protein on photoreceptor outer segment disk membranes that migrates a retinoid cycle product, *N*-retinyl-phosphatidylethanolamine (NR-PE), to the cytoplasmic surface where it can be recycled. If this process is interrupted by defective or absent function of the ATP-binding cassette transporter, NR-PE and its metabolites can accumulate within photoreceptor outer segments, which are then removed by RPE cells by phagocytosis and converted into lipofuscin.[26–28] This may spare the photoreceptors toxicity at the expense of the RPE, and this is consistent with the diffuse lipofuscin accumulation within the RPE observed angiographically as blocked choroidal fluorescence in Stargardt disease.[29] In most types of Stargardt disease, foveal RPE atrophy, often immediately surrounded by a ring of lipofuscin flecks, ensues with sufficient lipofuscin toxicity. However, SD-OCT and FAF findings from our cohort indicate that at least initially foveal cone photoreceptor dysfunction and atrophy occurs in the absence of RPE atrophy in Type 1 Stargardt disease. Although our series may not encompass all presentations of Type 1 Stargardt disease, we believe there is sufficient representation for further extrapolation. Several possible explanations may account for the findings observed in this cohort.

The absence of lipofuscin flecks within the RPE in Type 1 Stargardt disease indicates that the photoreceptor turnover of retinoid cycle products by the RPE is reduced, presumably from reduced phototransduction by foveal photoreceptors. Indeed, the first discernable sign of Type 1 Stargardt disease is diminished foveolar FAF, an indicator of retinoid cycle function and lipofuscin production. This correlates functionally with the observed central cone dysfunction by mfERG testing. However, SD-OCT was more useful than FAF or FA to determine the presence of RPE atrophy when photoreceptor atrophy was already present.[30,31] Fundus autofluorescence was reduced from photoreceptor dysfunction or atrophy alone, and FA demonstrated window defects even without RPE atrophy, although the intensity of hyperfluorescence increased further with RPE atrophy.

Accumulation of retinoid cycle byproducts results in structural changes in the photoreceptors early in the disease discernable by SD-OCT.[4,32] First, outer

Table 3. Proposed Staging System for Type 1 Stargardt Disease Resembling OMD and Corresponding SD-OCT and FAF Findings

Stage	SD-OCT Findings	FAF Findings
1	Hyperreflectivity of foveolar ONL and ELM Disruption of the inner segment ellipsoid band	Ovoid foveolar ↓FAF
2	Nonconfluent loss of foveolar cone OS Thinning of ONL but cell bodies intact	Ovoid foveolar ↓FAF
3	Loss of foveal cone OS Severe ONL thinning with loss of cell bodies	Ovoid foveal ↓FAF Surrounding ring of ↑FAF
4	Collapse of potential space (foveal cavitation) Merging of ELM to RPE	Ovoid foveal ↓FAF with Surrounding ring of ↑FAF
5*	Irregular thickening of subfoveal RPE Minimal transmission defects into choroid	Punctate ↑FAF around ovoid foveal ↓FAF
6*	Foveal and parafoveal retinal and RPE thinning and atrophy surrounded by irregular RPE thickening Transmission defects into choroid are present	Large central bull's eye lesion Extensive ↑FAF flecks

*Clinically identical to Type 2 Stargardt disease.
ELM, external limiting membrane; ↑FAF, hyperautofluorescence; ↓FAF, hypoautofluorescence; ONL, outer nuclear layer; OS, outer segments.

segment disorganization is evident by blurring and increased hyperreflectivity of the inner segment ellipsoid band. Later, outer segments become truncated as they lose contact with the RPE. Presumably, this results in decreased RPE phagocytosis of outer segments laden with retinoid cycle products. Otherwise FAF would remain unchanged or even increased. Instead, accumulated NR-PE or its toxic metabolites lead to photoreceptor apoptosis, evident by the gradual loss of foveal outer nuclear layer volume on SD-OCT. The Müller cell framework remains intact such that foveal cavitation is observed on SD-OCT. Eventually this potential space collapses as the external limiting membrane joins the RPE band, and RPE cell death and atrophy ensue, as in other photoreceptor dystrophies.

Animal models have demonstrated greater photoreceptor toxicity in cones compared with rods in ABCA4 knockouts because A2E may remain abnormally associated with cone photoreceptors, even in inner segments, where it would exert cytotoxic effects.[6] Although ABCA4 mutations affect both rod and cone photoreceptors, accumulation of A2E, and therefore lipofuscin, would be greatest in the macula, where cones are most densely crowded although RPE distribution remains uniform. Because the plasma membrane of cone outer segments is composed of redundant folds as opposed to discrete stacks of discs within a cylindrical plasma membrane, as in rods, misfolded ATP-binding cassette transporter may more greatly interfere with cone outer segment disk orientation and elongation compared with rods, and especially at the tightly packed foveola.[32] All patients in our series had one nonsense mutation and one missense mutation in ABCA4. More severe mutations in ABCA4 would be expected to result in greater cone and rod dysfunction on ffERG and express more peripheral distribution of lipofuscin flecks, and this is observed clinically in Types 2 and 3 Stargardt disease and ABCA4-mediated forms of cone–rod dystrophy and retinitis pigmentosa.[8] It remains unclear why patients with fundus flavimaculatus (Type 4 Stargardt disease) have foveal sparing initially in the disease.[14]

Functional and anatomical characteristics of our cohort with Type 1 Stargardt disease more closely resembled OMD, a central localized form of cone dystrophy, than other forms of macular degeneration, pattern dystrophy, or photoreceptor dystrophies.[7,30,33–39] Multifocal electroretinography revealed central cone dysfunction while ffERG demonstrated preserved generalized cone and rod function. The RP1L1 gene, responsible for hereditary cases of OMD, has been implicated in maintaining photoreceptor outer segment organization and length.[40] Conversely, its absence may result in disruption of the inner segment ellipsoid band, shortened outer segments, and foveal cavitation in eyes with OMD. We observed similar findings in patients with varying compound heterozygous ABCA4 mutations with Type 1 Stargardt disease. Several patients had a Gly1961Glc mutation, which has been previously reported to produce foveal cavitation, a nonspecific sign of central cone dysfunction.[37,39] These findings suggest that ABCA4 plays a role in maintaining photoreceptor outer segment organization and that toxicity from retinoid cycle products may inhibit outer segment production and photoreceptor viability. Alternatively, a secondary gene pathway may mediate cone dysfunction resembling OMD in patients with Type 1 Stargardt disease.

The relative preservation of foveal cone photoreceptor function in Type 4 disease compared with Type 1 disease further suggests a second pathway may

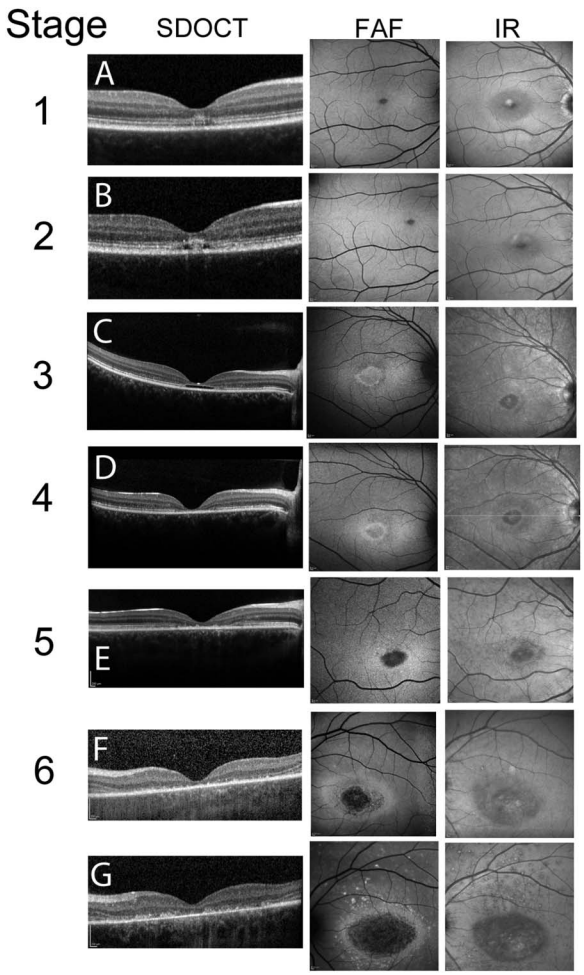

Fig. 2. Staging system for Type 1 Stargardt disease and corresponding multimodal imaging. **A.** Stage 1— the right macula of Patient 1 shows hyperreflectivity of foveolar outer nuclear layer and external limiting membrane with disruption of the inner segment ellipsoid band associated with foveolar oval area of hypoautofluorescence and corresponding subtle abnormality on infrared imaging (IR) masked by scanning laser reflex artifact. Note the absence of normal gradual transition from foveal hypoautofluorescence to isoautofluorescence associated with absorption of the excitation beam by luteal pigments. **B.** Stage 2—images of the right macula 6 months later in Patient 6 demonstrate the loss of foveal outer segments accompanying thinning of outer nuclear layer, although FAF and IR imaging remain unchanged. **C.** Stage 3—the right macula of Patient 1 shows the severe loss of photoreceptor tissue at the fovea despite normal-appearing RPE layer, resulting in foveal cavitation. Fundus autofluorescence and IR now demonstrate an enlarged bull's eye lesion with central isoautofluorescence. **D.** Stage 4—2 years later, the right macula of Patient 1 has collapse of the potential space but preservation of RPE thickness and the absence of transmission defects into the choroid. Foveal FAF becomes significantly reduced and IR imaging displays darker outer ring in bull's eye lesion. **E.** Stage 5—Raster scan of Patient 5 400 μm eccentric superiorly from the foveal center demonstrates irregular RPE thickening and rare transmission defects into the choroid. Punctate hyperautofluorescent dots begin to form around the fovea, and the outer ring on IR imaging appears coarser. **F** and **G.** Stage 6—the left macula of Patient 3 over 1 year of follow-up demonstrates progressive RPE atrophy and greater irregularity from lipofuscin clumping associated with very coarse foveal and parafoveal hypoautofluorescence surrounded by greatly expanded ring of hyperautofluorescence. Flecks throughout the macula become prominent both on FAF and IR imaging because only FAF imaging provides an indication of photoreceptor turnover, lipofuscin accumulation, and metabolic stress on the RPE, although the flecks appear more discretely on IR.

influence phenotype expression in Stargardt disease.[14] In contrast to patients with Type 1 disease, who presented within the first 2 decades, those with Type 4 disease typically presented later in life, after peripheral flecks have formed, supporting a protective mechanism for foveal cone photoreceptors in Type 4 disease or a second deleterious gene in other types of Stargardt disease. Although more peripheral distribution of lipofuscin flecks correlates with more extensive photoreceptor dysfunction, especially rod dysfunction, in other types of Stargardt disease, electrophysiologic activity and macular function are preserved in Type 4 disease.[41] Pathophysiologic studies of patients with Type 1 disease have demonstrated lipofuscin-engorged RPE cells. Furthermore, FA demonstrates blocked choroidal fluorescence and FAF imaging shows increased background FAF intensity compared with normal eyes, indicating widespread lipofuscin accumulation. Rather than the normal gradual transition of foveal hypoautofluorescence observed from absorption of the confocal scanning laser ophthalmoscope's excitation beam by luteal pigments, the transition is abrupt between the uniform background FAF and foveal hypoautofluorescence. Foveal hypoautofluorescence was observed only in the distribution of the photoreceptor outer segment defects by SD-OCT. Oxidative damage from accumulated retinoid cycle products may deplete luteal pigments despite leaving the intact Müller cell framework that affords the observed foveal cavitation.

The findings of this study challenge the accepted theory that phenotypic variability in Stargardt disease can solely be attributed to the degree of ABCA4 function or that Gass' types are segregated disease pathways.[7,42–48] Instead, it seems that patients who begin with Type 1 disease may evolve into Type 2 disease over time.[49,50] We hypothesize that the phenotypic variability in Stargardt disease is influenced by interactions with other genes to produce varying degrees of photoreceptor dysfunction and RPE lipofuscin accumulation.[51] Such digenic interactions and phenotypic variability have been documented among families with RDS-peripherin mutations.[52,53] We are currently investigating this hypothesis by testing for genes associated with age-related macular degeneration in patients with each type of Stargardt disease.

At the time of this publication, a Phase I human gene replacement therapy trial is currently enrolling for patients with Stargardt disease. In contrast to other phenotypes of Stargardt disease where foveal RPE atrophy occurs early in the disease, patients with Type 1 or Type 4 Stargardt disease may be particularly suitable candidates for this application if it is safe and efficacious because both photoreceptor cell bodies and

the RPE layer may be intact or salvageable.[54–58] Although an intact Müller cell framework integrated with photoreceptor cell bodies may resist macular hole formation or loss of cone outer segments or cell bodies associated with subretinal injection more than a thin, disorganized retinal remnant, an intravitreal procedure may provide a safer approach. Although most probands in our cohort had significant visual impairment at their initial diagnosis, symptoms began several years earlier. Screening of siblings led to an early diagnosis in two patients who should be more amenable to treatment. We hope the findings of this report and the ubiquitous use of SD-OCT and FAF among eye care specialists may facilitate earlier diagnostic recognition of Stargardt disease and subsequent treatment to preserve greater visual potential through gene replacement therapy or other emerging modalities.

Key words: cone dystrophy, fundus autofluorescence, infrared imaging, multifocal electroretinography, occult macular dystrophy, spectral domain optical coherence tomography, Stargardt disease.

References

1. Blacharski PA. Fundus flavimaculatus. In: Newsom DA, ed. Retinal Dystrophies and Degenerations. New York, NY: Raven Press; 1988:135–139.
2. Sun H, Nathans J. Mechanistic studies of ABCR, the ABC transporter in photoreceptor outer segments responsible for autosomal recessive Stargardt disease. J Bioenerg Biomembr 2001;33:523–530.
3. Sullivan JM. Focus on molecules: ABCA4 (ABCR)—an import-directed photoreceptor retinoid flippase. Exp Eye Res 2009;89:602–603.
4. Chen Y, Ratnam K, Sundquist SM, et al. Cone photoreceptor abnormalities correlate with vision loss in patients with Stargardt disease. Invest Ophthalmol Vis Sci 2011;52:3281–3292.
5. Molday LL, Rabin AR, Moday RS. ABCR expression in foveal cone photoreceptors and its role in Stargardt macular dystrophy. Nat Genet 2000;25:257–258.
6. Conley SM, Cai X, Makkia R, et al. Increased cone sensitivity to ABCA4 deficiency provides insight into macular vision loss in Stargardt's dystrophy. Biochim Biophys Acta 2012;1822: 1169–1179.
7. Gerth C, Andrassi-Darida M, Bock M, et al. Phenotypes of 16 Stargardt macular dystrophy/fundus flavimaculatus patients with known ABCA4 mutations and evaluation of genotype-phenotype correlations. Graefes Arch Clin Exp Ophthalmol 2002;240:628–638.
8. Cremers FP, vn de Pol DJ, van Driel M, et al. Autosomal recessive retinitis pigmentosa and cone-rod dystrophy caused by splice site mutations in the Stargardt's disease gene ABCR. Hum Mol Genet 1998;7:355–362.
9. Maugeri A, Klevering BJ, Rohrschneider K, et al. Mutations in the ABCA4 (ABCR) gene are the major cause of autosomal recessive cone-rod dystrophy. Am J Hum Genet 2000;67:960–966.
10. Martinez-Mir A, Paloma E, Allikmets R, et al. Retinitis pigmentosa caused by a homozygous mutation in the Stargardt disease gene ABCR. Nat Genet 1998;18:11–12.
11. Allikmets R, Shroyer NF, Singh N, et al. Mutation in the Stargardt disease (ABCR) in age-related macular degeneration. Science 1997;277:1805–1807.
12. Maugeri A, van Driel MA, van der Pol DJ, et al. The 2588G→C mutation in the ABCR gene is a mild frequent founder mutation in the Western European population and allows the classification of ABCR mutations in patients with Stargardt disease. Am J Hum Genet 1999;64:1024–1035.
13. Maugeri A, Flothmann K, Hemmrich N, et al. The ABCA4 2588G→C Stargardt mutation: single origin and increasing frequency from South-West to North-East Europe. Eur J Hum Genet 2002;10:197–203.
14. Westeneng-van Haaften SC, Boon CJF, Cremers FPM, et al. Clinical and genetic characteristics of late-onset Stargardt's disease. Ophthalmology 2012;119:1199–1210.
15. Jaakson K, Zernant J, Külm M, et al. Genotyping microarray (gene chip) for the ABCR (ABCA4) gene. Hum Mutat 2003; 22:395–403.
16. Yatsenko AN, Shroyer NF, Lewis RA, Lupski JR. Late-onset Stargardt disease is associated with missense mutations that map outside known functional regions of ABCR (ABCA4). Hum Genet 2001;108:346–355.
17. Cideciyan AV, Swider M, Aleman TS, et al. ABCA4 disease progression and a proposed strategy for gene therapy. Hum Mol Genet 2009;18:931–941.
18. Fishman GA, Stone EM, Grover S, et al. Variation of clinical expression in patients with Stargardt dystrophy and sequence variations in the ABCR gene. Arch Ophthalmol 1999;117: 504–510.
19. Zahid S, Jayasundera T, Rhoades W, et al. Clinical phenotypes and prognostic full-field electroretinographic findings in Stargardt disease. Am J Ophthalmol 2013;155:465–473.
20. Aaberg TM. Stargardt's disease and fundus flavimaculatus: evaluation of morphologic progression and intrafamilial coexistence. Trans Am Ophthalmol Soc 1986;84:453–487.
21. Gass JDM. Stereoscopic Atlas of Macular Diseases: Diagnosis and Treatment. 4th ed. Mosby; 1996.
22. Testa F, Maguire AM, Rossi S, et al. Three-year follow-up after unilateral subretinal delivery of adeno-associated virus in patients with Leber congenital amaurosis type 2. Ophthalmology 2013. Epub ahead of print.
23. Maguire AM, High KA, Auricchio A, et al. Age-dependent effects of RPE65 gene therapy for Leber's congenital amaurosis: a phase 1 dose-escalation trial. Lancet 2009;374:1597–1605.
24. Marmor MF, Fulton AB, Holder GE, et al. ISCEV standard for full-field clinical electroretinography (2008 update). Doc Ophthalmol 2008;118:69–77.
25. Hood DC, Bach M, Brigell M, et al. ISCEV standard for clinical multifocal electroretinography (mfERG) (2011 edition). Doc Ophthalmol 2012;124:1–13.
26. Molday RS. ATP-binding cassette transporter ABCA4: molecular properties and role in vision and macular degeneration. J Bioenerg Biomembr 2007;39:507–517.
27. Weng J, Mata NL, Azarian SM, et al. Insights into the function of Rim protein in photoreceptors and etiology of Stargardt's disease from the phenotype in abcr knockout mice. Cell 1999; 98:13–23.
28. Sparrow JR, Nakanishi K, Parish CA. The lipofuscin fluorophore A2E mediates blue light-induced damage to retinal pigmented epithelial cells. Invest Ophthalmol Vis Sci 2000;41: 1981–1989.
29. Ben-Shabat S, Parish CA, Vollmer HR, et al. Biosynthetic studies of A2E, a major fluorophore of retinal pigment epithelial lipofuscin. J Biol Chem 2002;277:7183–7190.

30. Gomez NL, Greenstein VC, Carlson JN, et al. A comparison of fundus autofluorescence and retinal structure in patients with Stargardt disease. Invest Ophthalmol Vis Sci 2009;50:3953–3959.
31. Fujinami KF, Tsunoda K, Hanazono G, et al. Fundus autofluorescence in autosomal dominant occult macular dystrophy. Arch Ophthalmol 2011;129:597–602.
32. Wiszniewski W, Zaremba CM, Yatsenko AN, et al. ABCA4 mutations causing mislocalization are found frequently in patients with severe retinal dystrophies. Hum Mol Genet 2005;14:2769–2778.
33. Hood DC, Zhang X, Ramachandran R, et al. The inner segment/outer segment border seen on optical coherence tomography is less intense in patients with diminished cone function. Invest Ophthalmol Vis Sci 2001;52:9703–9709.
34. Park SJ, Woo SJ, Park KH, et al. Morphologic photoreceptor abnormality in occult macular dystrophy on spectral-domain optical coherence tomography. Invest Ophthalmol Vis Sci 2010;51:3673–3679.
35. Kim Y-G, Baek S-H, Moon SW, et al. Analysis of spectral domain optical coherence tomography findings in occult macular dystrophy. Acta Ophthalmol 2001;89:e52–e56.
36. Kitaguchi Y, Kusaka S, Yamaguchi T, et al. Detection of photoreceptor disruption by adaptive optics fundus imaging and Fourier-domain optical coherence tomography in eyes with occult macular dystrophy. Clin Ophthalmol 2011;5:345–351.
37. Leng T, Marmor MF, Kellner U, et al. Foveal cavitation as an optical coherence tomography finding in central cone dysfunction. Retina 2012;32:1411–1419.
38. Kellner U, Kellner S. Clinical findings and diagnostics of cone dystrophy. Ophthalmologe 2009;106:99–108.
39. Cella W, Greenstein VC, Zernant-Rajang J, et al. G1961E mutant allele in the Stargardt disease gene ABCA4 causes bull's eye maculopathy. Exp Eye Res 2009;89:16–24.
40. Akahori M, Tsunoda K, Miyake Y, et al. Dominant mutations in RP1L1 are responsible for occult macular dystrophy. Am J Hum Genet 2010;87:424–429.
41. Armstrong JD, Meyer D, Xu S, Elfervig JL. Long-term follow-up of Stargardt's disease and fundus flavimaculatus. Ophthalmology 1998;105:448–457.
42. Simonelli F, Test A, Zernant J, et al. Genotype-phenotype correlation in Italian families with Stargardt disease. Ophthalmic Res 2005;37:159–167.
43. Paloma E, Coco R, Martinez-Mur A, et al. Analysis of ABCA4 in mixed Spanish families segregating different retinal dystrophies. Hum Mutan 2002;20:476.
44. Lewis RA, Shroyer NF, Singh N, et al. Genotype/Phenotype analysis of a photoreceptor-specific ATP-binding cassette transporter gene, ABCR, in Stargardt disease. Am J Hum Genet 1999;64:422–434.
45. Burke TR, Tsang SH, Zernant J, et al. Familial discordance in Stargardt disease. Mol Vis 2012;18:227–233.
46. Lois N, Holder GE, Fitzke FW, et al. Intrafamilial variation of phenotype in Stargardt macular dystrophy-fundus flavimaculatus. Invest Ophthalmol Vis Sci 1999;40:2668–2675.
47. Briggs CE, Rucinski D, Rosenfeld PJ, et al. Mutations in ABCR (ABCA4) in patients with Stargardt macular degeneration or cone-rod degeneration. Invest Ophthalmol Vis Sci 2001;42:2229–2236.
48. Maia-Lopes S, Silva ED, Silva MF, et al. Evidence of widespread retinal dysfunction in patients with Stargardt disease and morphologically unaffected carrier relatives. Invest Ophthalmol Vis Sci 2008;49:1191–1199.
49. Cukras CA, Wong WT, Caruso R, et al. Centrifugal expansion of fundus autofluorescence patterns in Stargardt disease over time. Arch Ophthalmol 2012;130:171–179.
50. Anastasakis A, Fishman GA, Lindeman M, et al. Infrared scanning laser ophthalmoscope imaging of the macula and its correlation with functional loss and structural changes in patients with Stargardt disease. Retina 2011;31:949–958.
51. Strom SP, Gao YQ, Martinez A, et al. Molecular diagnosis of putative Stargardt disease probands by exome sequencing. BMC Med Genet 2012;13:67.
52. Poloschek CM, Bach M, Lagreze WA, et al. ABCA4 and ROM1: implications for modification of the PRPH2-associated macular dystrophy phenotype. Invest Ophthalmol Vis Sci 2010; 51:4253–4265.
53. Boon CJF, den Hollander AI, Hoyng CB, et al. The spectrum of retinal dystrophies caused by mutations in the peripherin/RDS gene. Prog Retin Eye Res 2008;27:213–235.
54. Testa F, Rossi S, Sodi A, et al. Correlation between photoreceptor layer integrity and visual function in patients with Stargardt disease: implications for gene therapy. Invest Ophthalmol Vis Sci 2012;53:4409–4415.
55. Cideciyan AV, Hufnagel RB, Carroll J, et al. Human cone visual pigment deletions spare sufficient photoreceptors to warrant gene therapy. Hum Gene Ther 2013;24:993–1006.
56. Jacobson SG, Cideciyan AV, Ratnakaram R, et al. Gene therapy for leber congenital amaurosis caused by RPE65 mutations: safety and efficacy in 15 children and adults followed up to 3 years. Arch Ophthalmol 2012;130:9–24.
57. Sugiyama T, Katsumura K, Nakamura K, et al. Effects of chymase on the macular region in monkeys and porcine muller cells: probable involvement of chymase in the onset of idiopathic macular holes. Ophthalmic Res 2006;38:201–208.
58. Gass JD. Müller cell cone, an overlooked part of the anatomy of the fovea centralis: hypotheses concerning its role in the pathogenesis of macular hole and foveomacualr retinoschisis. Arch Ophthalmol 1999;117:821–823.